Comparing Electrical Magnetochiral Anisotropy and Chirality-Induced Spin Selectivity

G L J A Rikken, N. Avarvari

Comparing Electrical Magnetochiral Anisotropy And Chirality-Induced Spin Selectivity

G.L.J.A. Rikken
Laboratoire National des Champs Magnétiques Intenses
UPR3228 CNRS/EMFL/INSA/UGA/UPS
Toulouse & Grenoble, France.
email: geert.rikken@lncmi.cnrs.fr

N. Avarvari
Univ. Angers, CNRS, MOLTECH-Anjou
SFR MATRIX, F-49000 Angers, France
email: narcis.avarvari@univ-angers.fr

October 30, 2023

Abstract

The combination of chirality and magnetism has steadily grown over the last decennia into an area of intense research which evolves around two distinct manifestations and in two non-overlapping communities: electrical magnetochiral anisotropy (eMChA) and chirality-induced spin-selectivity (CISS). Here we discuss the similarities and differences of these two effects. Whereas the original CISS reports suggest an intimate relation with eMChA, magneto-resistance (MR) results on two-terminal chiral devices attributed to CISS, have symmetry properties that are different from those of eMChA. At the same time, the magnitudes of CISS MR and eMChA turn out to be similar when normalized to current density and spin polarization, suggesting a common underlying mechanism.

J. Phys. Chem. Lett. 2023, **14**, 9727-9731,
https://doi.org/10.1021/acs.jpclett.3c02546

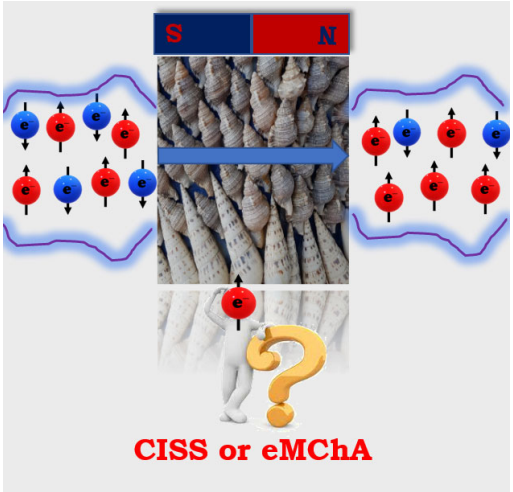

TOC Graphic

Chirality is vital in many areas of physics, chemistry and biology, where entities exist in two non-superimposable forms (enantiomers), one being the mirror image of the other. Since the time of Pasteur, the interplay between chirality and magnetism has been attracting much attention as a source of emergent phenomena. Fundamental symmetry arguments show that when a chiral system is placed in a magnetic field, a whole new family of effects, called magnetochiral anisotropies (MChA), becomes allowed (for a recent review, see[1]). The first member of this family to be experimentally reported, optical MChA, corresponds to a difference in the absorption and refraction of unpolarized light propagating parallel or anti-parallel to the field,[2].[3] Initially observed in the visible wavelength range,[4],[5],[6] its existence was later confirmed across the entire electromagnetic spectrum, from microwaves,[7][8] to X-rays,[9][10] and in photochemistry.[11] Electrical MChA (eMChA), was subsequently experimentally observed in the electrical resistance of bismuth helices,[12] carbon nano tubes,[13] bulk organic conductors,[14] metals,[15],[16] semiconductors[17] and superconductors[18] as a resistance R that depends on the handedness of the conductor and on the relative orientation of electrical current $\mathbf{I}$ and magnetic field $\mathbf{B}$, given to first order by

$$R^{D/L}(\mathbf{B},\mathbf{I}) = R_0(1+\gamma^{D/L}\mathbf{B}\cdot\mathbf{I}) \tag{1}$$

where $\gamma^D = -\gamma^L$ refers to the right/left-handed enantiomer of the conductor. In the case of a ferromagnetic material, it is more meaningful to express eMChA in terms of the magnetization $\mathbf{M}$ or the spin polarization $\mathbf{S}$ instead of the magnetic field $\mathbf{B}$.[16] A special case of electrical MChA is dielectric MChA that was observed in the displacement current in chiral ferroelectrics.[19] The latest addition to the MChA family, phonon MChA, was recently observed in the propagation of ultrasound,[20] further illustrating the universality of the phenomenon. MChA has become a prominent representative of the wider class of

non-reciprocal transport phenomena in broken-symmetry systems, that play an important role in topological quantum systems and in Berry phase physics,[21] an area that is currently intensively studied by condensed matter physicists.

The other main manifestation of the combined effect of chirality and magnetism is the so-called chirality-induced spin selectivity (CISS) (for a recent review see[22]). The first indication of CISS was observed in the transmission of spin-polarized photoelectrons from a gold substrate through chiral molecular layers.[23] CISS was explicitly established to depend on the handedness of the molecules[23] and on the spin polarization $\mathbf{S}$.[24] The model presented for CISS is that of spin-filtering, where the spin- and chirality-dependent electron transmission coefficient T through the chiral layer is expressed to first order as

$$T^{D/L}(\mathbf{S},\mathbf{v}) = T_0\left(1+\chi^{D/L}\mathbf{S}\cdot\mathbf{v}\right) \tag{2}$$

where $\chi^D = -\chi^L$ describes the chirality of the molecular layer and $\mathbf{v}$ is the charge velocity. Note that the dependence on $\mathbf{v}$ was not explicitly verified in the original CISS experiments, but is generally assumed in the explanations of the CISS effect.[22] The underlying physical picture for eMChA and for CISS is therefore the same: a charge carrier that moves through a medium and that has a longitudinal spin or orbital magnetic moment is chiral, and its chirality relative to that of the medium determines its interaction with that medium. (Strictly speaking a translating and spinning particle has helicity, but when considered in the molecular rest frame, chirality and helicity are equivalent.) Eq. 2 is clearly analogous to Eq. 1 as a magnetic field and spin polarization have the same parity-time (P-T) symmetry, and likewise for a current and a velocity. The second terms on the right-hand sides of both equations are therefore invariant under time-reversal and parity, i.e. fully symmetry allowed. CISS can therefore be regarded as a form of eMChA that is limited to the spin magnetic moment of charge carriers. Whereas MChA manifestations are generally quite weak, very strong CISS was observed, but so far no convincing quantitative theory has been put forward that explains the strength of the observed effect, the obvious coupling between chirality and spin through spin-orbit coupling being very weak in organic molecules (for a recent review see[25]). CISS has become a very active research topic in physical chemistry and biology, and more recently several other fascinating and strong manifestations of CISS were reported, ranging from magnetization reversal by the absorption of chiral molecules on a ferromagnet,[26] to chiral separations by flowing a chiral solution over a ferromagnetic substrate.[27]

The potential application of CISS in spintronics has also spurred a lot of activity (for a recent review see[28]). In particular, two-terminal devices consisting of chiral molecular layers between ferromagnetic contacts have shown quite strong effects,[29],[30],[31],[32],[33],[34].[35] Some discussion as to the possible role of CISS in such observations has arisen,[36][37] but most experimental reports agree on the phenomenology of anti-symmetric I-V curves, where the current is an odd function of the voltage **(i.e. I(V) = -I(-V))**, that are different for the two directions of longitudinal magnetization of the ferromagnetic contacts and that are different for the two handednesses of the chiral layer. It should be noted

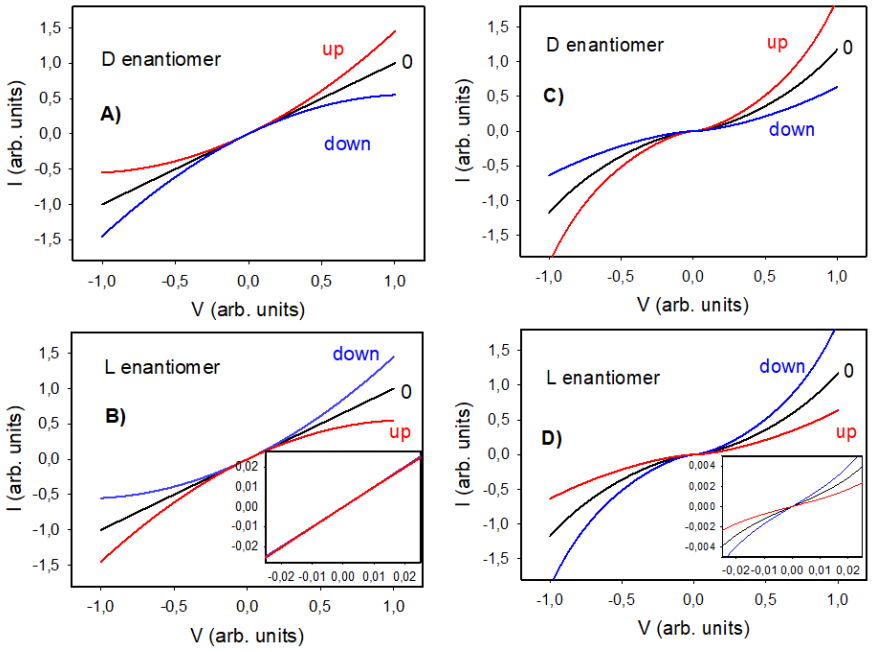

Figure 1: Schematic I-V characteristics of eMChA (A and B, strength exaggerated) and CISS MR (C and D) for both enantiomers (L/D) and magnetic field/spin polarization directions (up/down). Insets zoom on zero crossings.

that a few diverging reports exist, both in junction devices[38] and in field effect transistors.[39] Some theoretical microscopic models also predict I-V curves that are strictly odd in V,[42] but other models predict 'eMChA-like' I-V curves that contain V-even terms[43] or both.[44] One recent model is based on eMChA to explain CISS-MR, giving also anti-symmetric I-V curves.[45] Fig. 1 schematically summarizes and compares eMChA and the dominant experimental CISS magneto-resistance (CISS-MR) results. As pointed out above, the original CISS reports and eMChA share the same P-T symmetry properties, but as can be seen from Fig. 1, the more recent CISS-MR reports on two-terminal devices clearly differ from eMChA, showing different symmetry properties and suggesting different microscopic mechanisms. The microscopic origin of CISS-MR is still under intense debate and an analysis of its symmetry properties can provide powerful constraints on any microscopic model. In the remainder we perform such an analysis and compare the intrinsic orders of magnitude of both effects.

Firstly it should be noted that for symmetrical devices, magnetic field dependent antisymmetric I-V curves as in Fig. 1 C and D are unphysical, as a simple rotation over 180° around an axis perpendicular to the current leaves the device structure and its I-V curves unchanged, but inverts the direction

of the magnetization. We must therefore conclude that device asymmetry is a necessary condition for anti-symmetric I-V curves like in Fig. 1 C. Note that such an asymmetry can result from two different electrodes, either different in composition or in geometry, as is often the case in CISS-MR experiments, but also from a polar molecular orientation in the chiral layer which may result unintentionally from the deposition process. Paradoxically, asymmetric tunnel structures generally lead to asymmetric I-V curves[46] which is at odds with Fig. 1 C. However such a deviation from anti-symmetric I-V curves may be below the experimental detection limit. To elucidate the role of device asymmetry in the CISS-MR results, CISS-MR experiments with two identical ferromagnetic contacts should be performed and very careful comparisons between the results for the two enantiomers should be performed, excluding all other differences than the chirality of the central layer.

Next we will consider the C-P-T (C charge conjugation) symmetries of both effects. For eMChA, C-symmetry is satisfied if the material parameter γ in Eq. 1 is even under charge inversion. Indeed, the microscopic model for eMChA in Te finds such behavior for γ.[17] Fig. 1 C and D however require the material/device parameter of CISS-MR to be odd under charge conjugation. So far, no microscopic model has adressed this aspect but it suggests a different origin for CISS-MR as compared to eMChA, or an additional necessary component.

Clearly CISS-MR breaks time-reversal symmetry, as changing both the current direction and the magnetic field/spin polarization direction for a given enantiomer does not yield the same $\partial I/\partial V$. This is not altogether surprising, because generally time-reversal symmetry is not preserved in macroscopic dissipative processes, as Ohm's law clearly demonstrates. For such a situation, one should resort to the Onsager reciprocal relation which states that, close to thermodynamic equilibrium, a diagonal transport coefficient, like an electrical conductivity, should be even under time-reversal, which means that for eMChA and for CISS-MR the resistance for *up* and *down* magnetization should be identical at very small bias. This is the case for eMChA, however, as can be seen in Fig.1 C and D, CISS-MR does not obey the Onsager relation as for a given enantiomer $\partial I/\partial V(I=0,up) \neq \partial I/\partial V(I=0,down)$ (see the inset in Fig. 1 D) as can be seen in Refs.,[29],[30],[33],[34] whilst most other publications do not allow to judge whether the Onsager relation is violated or not. One clear observation of Onsager invariance in a CISS-MR experiment has been reported, albeit with the magnetization perpendicular to the current, which is not the normal CISS-MR configuration.[40] The Onsager reciprocal relation has been experimentally verified for diffusive transport,[41] but to our knowledge no theoretical justification nor any experimental verification for the case of tunneling or any other form of charge transport has been reported. Therefore, as an explanation for the apparent violation of Onsager non-reciprocity by CISS-MR close to thermal equilibrium, one must conclude that the Onsager relation does not apply to the electrical transport in CISS-MR devices with thin chiral layers, implying that this transport is not diffusive. Such an explanation would be consistent with recent observations of CISS-MR in macroscopic chiral field-effect devices, which are clearly in the diffusive transport regime, and where 'eMChA-like' asymmetry

in the I-V curves is reported.[39]

Apart from an effect of the electroweak force, which we can safely ignore here, no uncertainty exists for the requirement of parity invariance for dissipative processes and CISS-MR, like it is the case for eMChA, should be invariant under parity. If the device structure is symmetrical, i.e. consists of a chiral layer sandwiched between two identical ferromagnetic layers, parity invariance requires that $\partial I/\partial V(D,+I) = \partial I/\partial V(L,-I)$ for each magnetic field/spin polarization direction. It can be easily seen from Fig. 1 C and D that for CISS-MR, this relation is not obeyed, whereas it is obeyed by eMChA in Fig. 1 A and B. If the CISS-MR device has any polar asymmetry along the current direction, e.g. two different contacts or a *polar* chiral layer, the above condition no longer holds, and the I-V curves in Fig. 1 C and D do not necessarily break parity. Again, device asymmetry appears as a necessary condition for the predominant CISS-MR results.

Whereas eMChA is fully C-P-T symmetry allowed, as is CISS as expressed by Eq. 2, the symmetry analysis above shows that the experimental CISS-MR claims are not conform with the original CISS concept, and they raise questions as to their origin. The violation of the Onsager reciprocity is suggestive of an intrinsic absence of thermodynamic equilibrium. One possibility could therefore be that the CISS-MR is the result of the falsely chiral action of $E \cdot S$ away from equilibrium, where E is the electric field across the junction, proportional to the voltage V, and S the electron spin, proportional to the magnetization M of the contacts, and not of the truly chiral action of $I \cdot S$.[47] The intrinsic out-of-equilibrium character of false chirality would then automatically explain why the Onsager relation does not apply to CISS-MR. However, in the case of false chirality, for a given chiral barrier, the response to $E \cdot S$ should be the same as that to $(\text{-}E) \cdot (-S)$ which is clearly not the case in Fig. 1 C or D. Although our translation of false chirality, as developed for chemical reactivity, into electrical transport may be subject to discussion, we arrive at the conclusion that false chirality does not seem able to explain these CISS-MR observations, unless a strong built-in electric field is present in these devices. The presence of such a field would however not be compatible with anti-symmetric I-V curves. The enantioseparation at ferromagnetic surfaces, which is also considered a manifestation of CISS,[27] is however fully compatible with false chirality.[48]

Another apparent difference between eMChA and CISS-MR lies in the magnitudes of the respective reported relative non-reciprocities $\eta_{eMChA} \equiv (R(+B)-R(-B))/R(B=0)$ and $\eta_{CISS} \equiv (R(+S)-R(-S))/R(S=0)$, the values for eMChA being several orders of magnitude smaller than the CISS-MR values. However, for a meaningful quantitative comparison, both should be normalized to the same current density J and to the same average magnetic polarization S of the charge carriers, i.e. one should compare $\widetilde{\eta} \equiv \eta/S/J$. Assuming simple Pauli paramagnetism for the conduction electrons, i.e. $S = (\mu_B B/kT)\mu_B \simeq 4,1\ 10^{-3}\mu_B$ in an external field of 1 T at room temperature, the eMChA results on [DM-EDT-TTF]$_2$ClO$_4$[14] and on Te[17] correspond to normalized relative non-reciprocity values $\widetilde{\eta}_{eMChA}$ of 5 10^{-8} $m^2/A/\mu_B$ and 1 10^{-6} $m^2/A/\mu_B$. respectively. Alternatively one could assume Landau dia-

magnetism for the conduction electrons, which would yield normalized non-reciprocity values that are a factor 3 larger, the Landau susceptibility being 3 times smaller than the Pauli susceptibility. For a typical CISS-MR result with ferromagnetic nickel contacts, a current density of $2\ 10^5\ A/m^2$ and a relative non-reciprocity of $1,5\%$,[30] and using $S \simeq 0,23\ {\mu_B}^{49}$ one finds a normalized $\widetilde{\eta}_{CISS} = 3\ 10^{-7}\ m^2/A/\mu_B$, i.e. of the same order of magnitude as $\widetilde{\eta}_{eMChA}$. In junctions using an atomic force microscope, much higher current densities can occur, resulting in very large η_{CISS} observed in such devices. Therefore we can conclude thateMChA and CISS-MR have very similar intrinsic magnitudes, and the apparent differences in strength only result from the different experimental configurations in which they are measured. Despite their different symmetry properties, identified above, this does point to a common underlying mechanism which would be consistent with the similarity in symmetry between eMChA and the original CISS observations. In particular, no exceptional spin-orbit coupling strength is required for CISS-MR.

Summarizing the analysis above, we can say that

i) the commonly observed magnetic field direction dependent antisymmetric CISS-MR I-V curves cannot solely be an expression of chirality but also require a polar asymmetry in the device, which is not compatible with the simplest possible interpretation of CISS-MR being a purely spin filtering effect, only dependent on the charge carrier's helicity as compared to the central layer's chirality. As most CISS-MR reports use different metals for the two contacts, this suggest that an interface effect could be important.

ii) the predominantly observed violation of the Onsager reciprocity relation excludes a diffusive transport mechanism and it is currently unknown how other transport mechanisms (tunneling, hopping, field emission,...) relate to Onsager reciprocity.

iii) the magneto-chiral material/device parameter should be odd in the charge of the charge carriers

iv) false chirality cannot be the explanation for the observed I-V curves

v) the intrinsic magnitudes of eMChA and CISS-MR, normalized for current density and magnetic polarization, are comparable

Although at a fundamental level, eMChA and CISS are very close, the first three points listed above for CISS-MR are at odds with eMChA, and require an enhanced model for CISS-MR, beyond the original CISS concept. Clearly there are basic issues to address for CISS-MR and we hope that the new insights presented here will contribute to developing a detailed understanding and identifying a microscopic model for CISS-MR.

Corresponding author
G.L.J.A. Rikken, geert.rikken@lncmi.cnrs.fr

Acknowledgements
This work was supported by the French National Agency for Research project SECRETS (ANR PRC 20-CE06-0023-01). We gratefully acknowledge helpful discussions with L. Barron.

References

1. Atzori, M.; Train, C.; Hillard, E. A.; Avarvari, N.; Rikken, G. L. J. A. Magnetochiral anisotropy: from fundamentals to perspectives. *Chirality* **2021**, 33, 844–857.

2. Wagnière, G.; Meier, A. The influence of a static magnetic field on the absorption coefficient of a chiral molecule. *Chem. Phys. Lett.* **1982**, 93, 78–81.

3. Barron, L. D.; Vrbancich, J. Magnetochiral birefringence and dichroism. *Mol. Phys.* **1984**, 51, 715–730.

4. Rikken, G. L. J. A.; Raupach, E. Observation of magneto-chiral dichroism. *Nature* **1997**, 390, 493–494.

5. Kleindienst, P.; Wagnière, G. H. Interferometric detection of magnetochiral birefringence. *Chem. Phys. Lett.* **1998**, 288, 89–97.

6. Rikken, G. L. J. A.; Raupach, E. Pure and cascaded magnetochiral anisotropy in optical absorption. *Phys. Rev. E* **1998**, 58, 5081–5084.

7. Tomita, S.; Sawada, K.; Porokhnyuk, A.; Ueda, T. Direct observation of magnetochiral effects through a single metamolecule in microwave regions. *Phys. Rev. Lett.* **2014**, 113, 235501.

8. Okamura, Y.; Kagawa, F.; Seki, S.; Kubota M.; Kawasaki, M.; Tokura, Y. Microwave magnetochiral dichroism in the chiral-lattice magnet Cu2OSeO3. *Phys. Rev. Lett.* **2015**, 114, 197202.

9. Ceolín, M.; Goberna-Ferrón, S.; Galán-Mascarós, J. R. Strong Hard X-ray Magnetochiral dichroism in paramagnetic enantiopure molecules. *Adv. Mater.* **2012**, 24, 3120–3123.

10. Sessoli, R.; Boulon, M.-E.; Caneschi, A.; Mannini, M.; Poggini, L.; Wilhelm, F.; Rogalev, A. Strong magnetochiral dichroism in a paramagnetic molecular helix observed by hard X-rays. *Nat. Phys.* **2015**, 11, 69–74.

11. Rikken, G. L. J. A.; Raupach, E. Enantioselective magnetochiral photochemistry, Nature 2000, 405, 932.

12. Rikken, G. L. J. A.; Fölling, J.; Wyder, P. Electrical Magnetochiral Anisotropy. *Phys. Rev. Lett.* **2001**, 87, 236602.

13. Krstić, V.; Roth, S.; Burghard, M.; Kern, K.; Rikken, G. L. J. A. Magnetochiral anisotropy in charge transport through single-walled carbon nanotubes. *J. Chem. Phys.* **2002**, 117, 11315–11319.

14. Pop, F.; Auban-Senzier, P.; Canadell, E.; Rikken, G. L. J. A.; Avarvari, N. Electrical magnetochiral anisotropy in a bulk chiral molecular conductor. *Nat. Commun.* **2014**, 5, 3757.

15. Yokouchi, T.; Kanazawa, N.; Kikkawa, A.; Morikawa, D.; Shibata, K.; Arima, T.; Taguchi, Y.; Kagawa, F.; Tokura, Y. Electrical magnetochiral effect induced by chiral spin fluctuations. *Nat. Commun.* **2017**, 8, 866.

16. Aoki, R.; Kousaka, Y.; Togawa, Y. Anomalous nonreciprocal electrical transport on chiral magnetic order. *Phys. Rev. Lett.* **2019**, 122, 057206.

17. Rikken, G. L. J. A.; Avarvari, N. Strong electrical magnetochiral anisotropy in tellurium. *Phys. Rev. B.* **2019**, 99, 245153.

18. Qin F.; Shi W.; Ideue T.; Yoshida M.; Zak A.; Tenne R.; Kikitsu T.; Inoue D.; Hashizume D.; Iwasa Y. Superconductivity in a chiral nanotube, *Nat. Commun.* **2017**, 8, 14465.

19. Rikken, G. L. J. A.; Avarvari, N. Dielectric Magnetochiral Anisotropy, *Nat. Commun.* **2022**, 13, 3564.

20. Nomura, T.; Zhang, X.-X.; Zherlitsyn, S.; Wosnitza, J.; Tokura, Y.; Nagaosa, N.; Seki, S. Phonon magnetochiral effect. *Phys. Rev. Lett.* **2019**, 122, 145901.

21. Tokura, Y.; Nagaosa, N. Nonreciprocal responses from noncentrosymmetric quantum materials. *Nat. Commun.* **2018**, 9, 3740.

22. Naaman, R.; Paltiel, Y.; Waldeck, D. H. Chiral molecules and the electron spin. *Nat. Rev. Chem.* **2019**, 3, 250–260.

23. Ray, K.; Ananthavel, S. P.; Waldeck, D. H.; Naaman, R. Asymmetric Scattering of Polarized Electrons by Organized Organic Films of Chiral Molecules. *Science* **1999**, 283, 814–816.

24. Göhler, B.; Hamelbeck, V.; Markus, T. Z.; Kettner, M.; Hanne, G. F.; Vager, Z.; Naaman, R.; Zacharias, H. Spin Selectivity in Electron Transmission Through Self-Assembled Monolayers of Double-Stranded DNA. *Science* **2011**, 331, 894–897.

25. Evers, F.; Aharony, A.; Bar-Gill, N.; Entin-Wohlman, O.; Hedegård, P.; Hod, O.; Jelinek, P.; Kamieniarz, G.; Lemeshko, M.; Michaeli, K.; Mujica, V.; Naaman, R.; Paltiel, Y.; Refaely-Abramson, S.; Tal, O.; Thijssen, J.; Thoss, M.; van Ruitenbeek, J. M.; Venkataraman, L.; Waldeck, D. H.; Yan, B.; Kronik, L. Theory of Chirality Induced Spin Selectivity: Progress and Challenges. *Adv. Mater.* **2022**, 34, 2106629.

26. Ben Dor, O.; Yochelis, S.; Radko, A.; Vankayala, K.; Capua, E.; Capua, A.; Yang, S.-H.; Baczewski, L. T.; Parkin, S. S. P.; Naaman, R.; Paltiel, Y. Magnetization switching in ferromagnets by adsorbed chiral molecules without current or external magnetic field. *Nat. Commun.* **2017**, 8, 14567

27. Banerjee-Ghosh, K.; Ben Dor, O.; Tassinari, F.; Capua, E.; Yochelis, S.; Capua, A.; Yang, S.-H.; Parkin, S. S. P.; Sarkar, S.; Kronik, L.; Baczewski, L. T.; Naaman, R.; Paltiel, Y. Separation of enantiomers by their enantiospecific interaction with achiral magnetic substrates. *Science* **2018**, 360, 1331–1334.

28. Yang, S.-H.; Naaman , R.; Paltiel, Y.; Parkin, S. S. P. Chiral spintronics. *Nat. Rev. Phys.* **2021**, 3, 328–343.

29. Alam, K. M.; Pramanik, S. Spin Filtering through Single-Wall Carbon Nanotubes Functionalized with Single-Stranded DNA. *Adv. Funct. Mater.* **2015**, 25, 3210–3218.

30. Kiran, V.; Mathew, S. P.; Cohen, S. R.; Hernández Delgado, I.; Lacour, J.; Naaman, R. Helicenes–A New Class of Organic Spin Filter. *Adv. Mater.* **2016**, 28, 1957–1962.

31. Lu, H.; Wang, J.; Xiao, C.; Pan, X.; Chen, X.; Brunecky, R.; Berry, J. J.; Zhu, K.; Beard, M. C.; Vardeny, Z. V.. Spin-dependent charge transport through 2D chiral hybrid lead-iodide perovskites. *Sci. Adv.* **2019**, 5, eaay0571.

32. Rahman M.W.; Mañas-Torres M.C.; Firouzeh S.; Cuerva J.M.,Álvarez de Cienfuegos L.; and Pramanik S. Molecular Functionalization and Emergence of Long-Range Spin-Dependent Phenomena in Two-Dimensional Carbon Nanotube Networks, *ACS Nano* **2021**, 15, 20056-20066.

33. Al-Bustami, H.; Khaldi, S.; Shoseyov, O.; Yochelis, S.; Killi, K.; Berg, I.; Gross, E.; Paltiel, Y.; Yerushalmi, R. Atomic and Molecular Layer Deposition of Chiral Thin Films Showing up to 99% Spin Selective Transport. *Nano Lett.* **2022**, 22, 5022–5028.

34. Amsallem, D.; Kumar, A.; Naaman, R.; Gidron, O. Spin polarization through axially chiral linkers: Length dependence and correlation with the dissymmetry factor. *Chirality* **2023**, 35, 562–568.

35. Aizawa, H.; Sato, T.; Maki-Yonekura, S.; Yonekura, K.; Takaba, K.; Hamaguchi, T.; Minato, T.; Yamamoto, H. M. Enantioselectivity of discretized helical supramolecule consisting of achiral cobalt phthalocyanines via chiral-induced spin selectivity effect. *Nat. Commun.* **2023**, 14, 4530.

36. Yang, X.; van der Wal, C. H.; van Wees, B. J. Spin-dependent electron transmission model for chiral molecules in mesoscopic devices. *Phys. Rev. B* **2019**, 99, 024418.

37. Naaman R.; Waldeck, D. H. Comment on "Spin-dependent electron transmission model for chiral molecules in mesoscopic devices". *Phys. Rev. B* **2020**, 101, 026403

38. Abendroth, J. M.; Cheung, K. M.; Stemer, D. M.; El Hadri, M. S.; Zhao, C.; Fullerton, E. E.; Weiss, P. S. Spin-Dependent Ionization of Chiral Molecular Films. *J. Am. Chem. Soc.* **2019**, 141, 3863–3874.

39. Volpi, M.; Jouclas, R.; Liu, J.; Liu, G.; Catalano, L.; McIntosh, N.; Bardini, M.; Gatsios, C.; Modesti, F.; Turetta, N.; Beljonne, D.; Cornil, J.; Kennedy, A. R.; Koch, N.; Erk, P.; Samorì, P.; Schweicher, G.; Geerts, Y. H. Enantiopure Dinaphtho[2,3-b:2,3-f]thieno[3,2-b]thiophenes: Reaching High Magnetoresistance Effect in OFETs. *Adv. Sci.* **2023**, 2301914.

40. Hossain, M.; Illescas-Lopez, S.; Nair, R.; Cuerva, J.; Alvarez de Cienfuegos, L.; Pramanik, S. Transverse magnetoconductance in two-terminal chiral spin-selective devices. *Nanoscale Horiz.* **2023**, 8, 320–330

41. Miller, D. G. The Onsager Relations; Experimental Evidence, in Foundations of Continuum Thermodynamics. p. 185 ff, eds. Delgado Domingos, J. J.; Nina, M. N. R.; Whitelaw, J. H. MacMillan, London, **1974**.

42. Huisman, K. H.; Heinisch, J.-B. M.-Y.; Thijssen, J. M. Chirality-Induced Spin Selectivity (CISS) Effect: Magnetocurrent-Voltage Characteristics with Coulomb Interactions. *J. Phys. Chem. C* **2023**, 127, 6900–6905.

43. Yang, X.; van der Wal, C. H.; van Wees, B. J. Detecting Chirality in Two-Terminal Electronic Nanodevices. *Nano Lett.* **2020**, 20, 6148–6154.

44. Huisman K. H.; Heinisch J. B. M. Y.; Thijssen J.M. CISS effect: Magnetocurrent–voltage characteristics with Coulomb interactions. II, J. Chem. Phys. 2023, 158, 174108.

45. Xiao J., Zhao Y.; Yan B. Nonreciprocal Nature and induced Tunneling Barrier Modulation in Chiral Molecular Devices, arXiv:2201.03623v2.

46. Choi, K.; Yesilkoy, F.; Ryu, G.; Cho, S. H.; Goldsman, N.; Dagenais, M.; Peckerar, M. A Focused Asymmetric Metal—Insulator—Metal Tunneling Diode: Fabrication, DC Characteristics and RF Rectification, *IEEE Trans. Electron. Dev.* **2011**, 58, 3519–3528.

47. Barron, L. D. Reactions of chiral molecules in the presence of a time-noninvariant enantiomorphous influence. *Chem. Phys. Lett.* **1987**, 135, 1–8.

48. Barron, L. D. Symmetry and Chirality: Where Physics Shakes Hands with Chemistry and Biology. *Isr. J. Chem.* **2021**, 61, 517–529.

49. Tedrow P. M.; Meservey, R. Spin polarized electron tunneling. *Phys. Rep.* **1994**, 238, 173–243.